

1 **Supplementary information**

2

3 **Thermal structure of the Venusian atmosphere from the sub-**

4 **cloud region to the mesosphere as observed by radio**

5 **occultation**

6 *Hiroki Ando¹ (hando@cc.kyoto-su.ac.jp), Takeshi Imamura², Silvia Tellmann³,

7 Martin Pätzold³, Bernd Häusler⁴, Norihiko Sugimoto⁵, Masahiro Takagi¹,

8 Hideo Sagawa¹, Sanjay Limaye⁶, Yoshihisa Matsuda⁷, Rajkumar Choudhary⁸ and

9 Maria Antonita⁹

10

11 1: Kyoto Sangyo University, 2: The University of Tokyo, 3: Universität zu Köln,

12 4: Universität der Bundeswehr München, 5: Keio University, 6: Keio University,

13 7: Tokyo Gakugei University, 8: Vikram Sarabhai Space Center,

14 9: Indian Space Research Organization

15

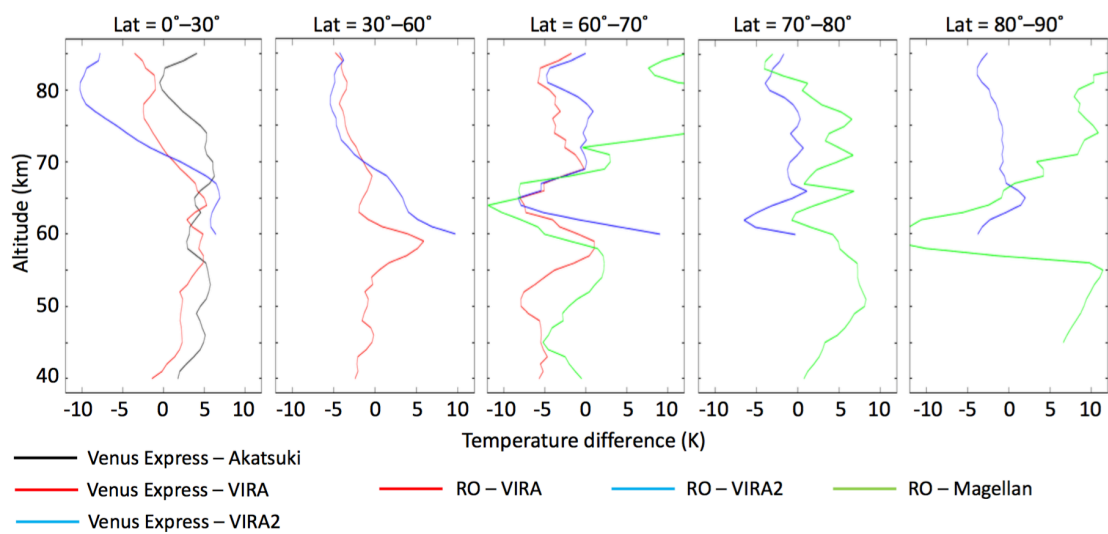
16

17 **1. Detail of the comparison of the temperature distributions obtained by the radio**

18 **occultation measurements, VIRA and VIRA-2**

19 Fig. S1 shows temperature differences among the radio occultation measurements,
20 VIRA and VIRA-2. Fig. S2 shows the temperature distributions obtained from the
21 Akatsuki and Venus Express radio occultation measurements. Although the temperature
22 obtained on the Akatsuki mission is 2–5 K lower than that obtained on the Venus
23 Express mission at all altitudes (see also Fig. S1), the shape and curvature of these
24 temperature profiles are similar. The static stabilities obtained from these radio
25 occultation measurements are then almost consistent as shown in Fig. S3.

26

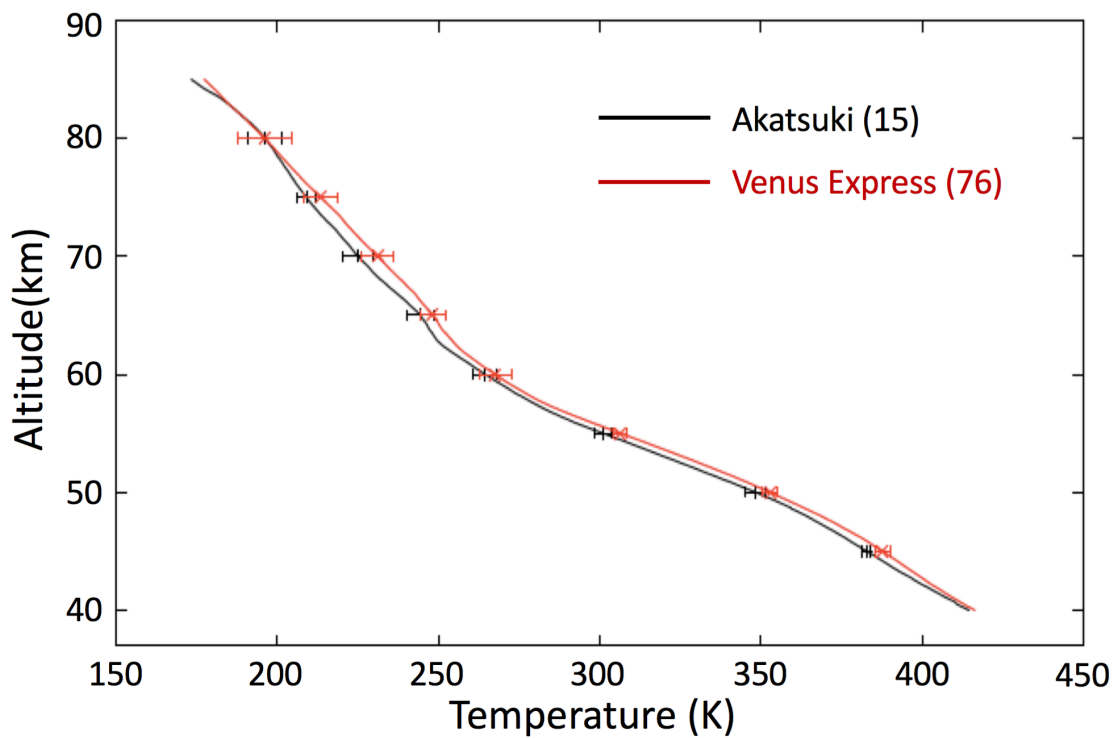


27

28 **Figure S1 | Differences in temperature among radio occultation measurements,**

29 **VIRA and VIRA-2.** At latitudes of 0° – 30° , the temperature differences between Venus
30 Express and Akatsuki (black), between Venus Express and VIRA (red), and between
31 Venus Express and VIRA-2 (blue) are shown. At other latitudes, the temperature
32 differences between the present study and VIRA (red) and between VIRA-2 (blue) and
33 Magellan radio occultation measurements (green) are shown.

34



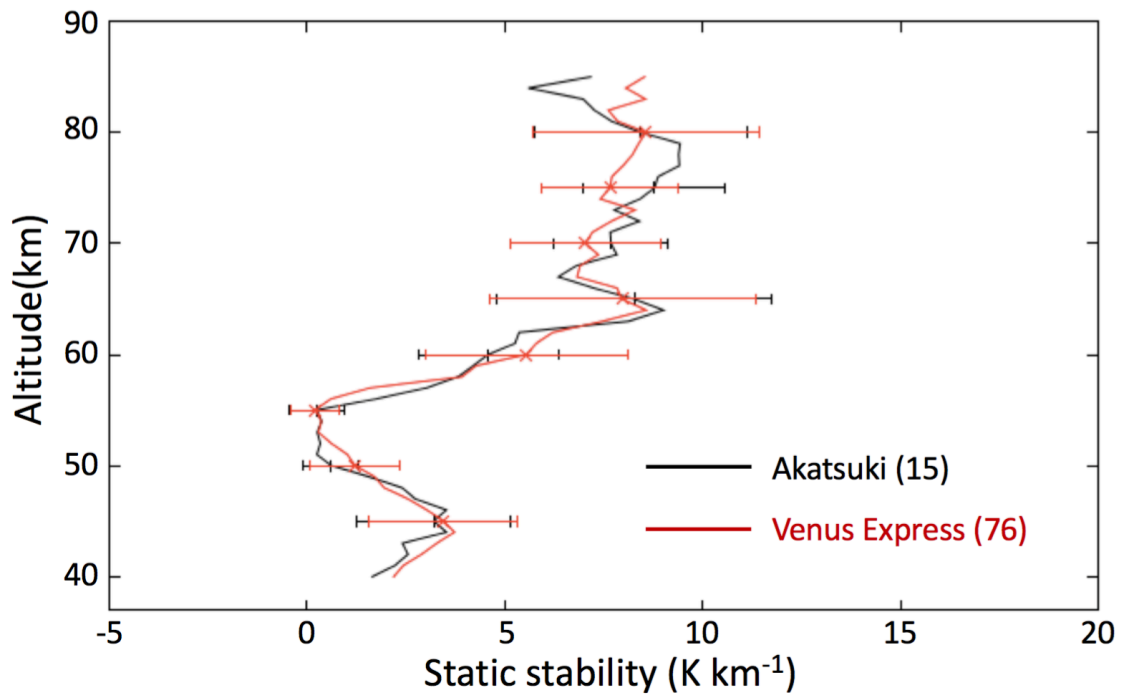
35

36 **Figure S2 | Comparison of mean temperatures at altitudes of 40–85 km for**
37 **latitudes of 0° – 30° obtained from radio occultation measurements made on (black)**
38 **Akatsuki and (red) Venus Express missions.** The number within parentheses in each

39 panel is the number of radio occultation measurements made at an altitude of 50 km. An

40 error bar represents the standard deviation of the temperature.

41



42

43 **Figure S3 | Comparison of mean static stabilities at altitudes of 40–85 km for**

44 **latitudes of 0°–30° obtained from radio occultation measurements made on (black)**

45 **Akatsuki and (red) Venus Express missions.** The number within parentheses in each

46 panel is the number of radio occultation data measurements made at an altitude of 50

47 km. An error bar represents the standard deviation of the temperature.

48

49 **2. Measurement error due to horizontal drift**

50 Venus Express had a polar orbit. Horizontal drift of the ray path tangent point thus
51 generated measurement error in the temperature at low latitudes. The error is estimated
52 here following the work of Kursinski et al. (1997).

53 The bending angle error, $\delta\alpha(z, z_0, y)$, due to horizontal drift of the ray path tangent
54 point is expressed to the first order as

55
$$\delta\alpha(z, z_0, y) = \Delta y(z, z_0, y) \frac{\partial\alpha}{\partial y}(z, y) , \quad (\text{A1})$$

56 where y represents latitude and z is the height of the error, z_0 is the altitude of the
57 lower integration limit of the Abel transform and the altitude of the refractivity retrieval,
58 and Δy is the horizontal distance that the ray path tangent point drifts between z and
59 z_0 . For simplicity, we assume that α is proportional to the vertical density gradient
60 such that $\alpha \sim c\rho/H$, where c is a scale factor, ρ is the mass density and $H = RT/g$
61 is the density scale height, with R , T and g respectively being the gas constant,
62 temperature and gravity acceleration. Making this assumption, it follows that

63
$$\frac{1}{\alpha} \frac{\partial\alpha}{\partial y}(z, y) \sim \frac{1}{\rho} \frac{\partial\rho}{\partial y}(z, y) - \frac{1}{T} \frac{\partial T}{\partial y}(z, y) . \quad (\text{A2})$$

64 In the case of Venus, the cyclostrophic balance can be applied as

65
$$\frac{u_c^2 \tan \varphi}{a} = -\frac{1}{\rho} \frac{\partial p}{\partial y}, \quad (\text{A3})$$

66 where a is the radius of Venus, u_c is the cyclostrophic wind, p is pressure and φ is the
67 latitude. Taking the vertical gradient of (A3) gives

68
$$\frac{\partial}{\partial z} \left(\frac{\rho u_c^2}{a} \right) = -\frac{1}{\tan \varphi} \frac{\partial}{\partial y} \left(\frac{\partial p}{\partial z} \right) = \frac{g}{\tan \varphi} \frac{\partial \rho}{\partial y}. \quad (\text{A4})$$

69 The first term on the right-hand side of (A2) can therefore be rewritten as

70
$$\frac{1}{\rho} \frac{\partial \rho}{\partial y} (z, y) = \frac{\tan \varphi}{ag} \left(2u_c \frac{\partial u_c}{\partial z} + \frac{u_c^2}{\rho} \frac{\partial \rho}{\partial z} \right) = \frac{\tan \varphi}{ag} \left(2u_c \frac{\partial u_c}{\partial z} - \frac{u_c^2}{H} \right). \quad (\text{A5})$$

71 The second term on the right-hand side of (A2) is related to the vertical gradient of the
72 cyclostrophic wind such that

73
$$\frac{\partial}{\partial z} \left(\frac{u_c^2 \tan \varphi}{a} \right) = -\frac{R}{H} \frac{\partial T}{\partial y} = -\frac{g}{T} \frac{\partial T}{\partial y}. \quad (\text{A6})$$

74 Accordingly, (A2) is finally described as

75
$$\frac{1}{\alpha} \frac{\partial \alpha}{\partial y} (z, y) = \frac{\tan \varphi}{ag} \left(4u_c \frac{\partial u_c}{\partial z} - \frac{u_c^2}{H} \right). \quad (\text{A7})$$

76 The fractional error in the bending angle due to horizontal drift of the ray path tangent
77 point is then written as

78
$$\frac{\delta \alpha}{\alpha} = \frac{\tan \varphi}{ag} \left(4u_c \frac{\partial u_c}{\partial z} - \frac{u_c^2}{H} \right) \Delta y. \quad (\text{A8})$$

79 The radius (a) is 6050 km, gravitational acceleration (g) is 8.87 m s^{-2} , the density scale
80 height (H) is fixed at 5 km and the latitude (φ) is fixed at 20° . We consider the two

81 altitude ranges of 40–50 km and 60–70 km. In the case of the Venus Express radio
82 occultation measurements made at low latitude, Δy is approximately 10^3 km at
83 altitudes of 40–50 km and 10^2 km at altitudes of 60–70 km, which corresponds to
84 latitudinal movement of $\sim 10^\circ$ and $\sim 1^\circ$, respectively. Inserting these values into (A8) to
85 calculate the temperature measurement error (δT) yields $\delta\alpha/\alpha \sim 6.7 \times 10^{-4}$ and $\delta T \sim$
86 0.05 K at altitudes of 40–50 km and $\delta\alpha/\alpha \sim 2.7 \times 10^{-4}$ and $\delta T \sim 0.03$ K at altitudes
87 of 60–70 km. These δT values are smaller than the measurement error of 0.1 K, which
88 is associated with the stability of the oscillator onboard the spacecraft.

89

90 **References**

91 Kursinski, E. R., Hajj, G. A., Schofield, J. T., Linfield, R. P. & Hardy, K. R. Observing
92 Earth's atmosphere with radio occultation measurements using the Global Positioning
93 System. *J. Geophys Res.* **102**, 23429–23466 (1997).

94

95 **Figure legends**

96 **Figure S1 | Differences in temperature among radio occultation measurements,**

97 **VIRA and VIRA-2.** At latitudes of 0° – 30° , the temperature differences between Venus
98 Express and Akatsuki (black), between Venus Express and VIRA (red), and between
99 Venus Express and VIRA-2 (blue) are shown. At other latitudes, the temperature
100 differences between the present study and VIRA (red) and between VIRA-2 (blue) and
101 Magellan radio occultation measurements (green) are shown.

102

103 **Figure S2 | Comparison of mean temperatures at altitudes of 40–85 km for**
104 **latitudes of 0° – 30° obtained from radio occultation measurements made on (black)**
105 **Akatsuki and (red) Venus Express missions.** The number within parentheses in each
106 panel is the number of radio occultation measurements made at an altitude of 50 km. An
107 error bar represents the standard deviation of the temperature.

108

109 **Figure S3 | Comparison of mean static stabilities at altitudes of 40–85 km for**
110 **latitudes of 0° – 30° obtained from radio occultation measurements made on (black)**
111 **Akatsuki and (red) Venus Express missions.** The number within parentheses in each
112 panel is the number of radio occultation data measurements made at an altitude of 50

113 km. An error bar represents the standard deviation of the temperature.